

Low Delay Rate Allocation in WLANs Using Aggregation

Francesco Gringoli, Douglas J. Leith

Abstract—In this paper we consider transport layer approaches for achieving high rate, low delay communication over edge paths where the bottleneck is a modern WLAN which can aggregate multiple packets into each WLAN frame. We show that regulating send rate so as to maintain a target aggregation level can be used to avoid queue buildup at the WLAN AP. We derive an approximate downlink throughput model for WLANs using aggregation, verify its accuracy using experimental measurements and using this determine a convex low delay rate region. This allows us to derive a low delay proportional fair rate allocation for which we present a prototype transport layer implementation.

1 INTRODUCTION

While much attention in 5G has been focussed on the physical and link layers, it is increasingly being realised that a wider redesign of network protocols is also needed in order to meet 5G requirements. Transport protocols are of particular relevance for end-to-end performance, including end-to-end latency. For example, ETSI has recently set up a working group to study next generation protocols for 5G [1]. The requirement for major upgrades to current transport protocols is also reflected in initiatives such as Google QUIC [2], Coded TCP [3] and the Open Fast Path Alliance [4].

In this paper we consider next generation edge transport architectures of the type illustrated in Figure 1. Traffic to and from client stations is routed via a proxy located close to the network edge (e.g. within a cloudlet). This creates the freedom to implement new transport layer behaviour over the path between proxy and clients, which in particular includes the last wireless hop. One great advantage of this architecture is its ease of rollout since the new transport can be implemented as an app on the clients and no changes are required to existing servers.

Our interest is in achieving high rate, low delay communication. One of the most challenging requirements in 5G is the provision of connections with low end-to-end latency. In most use cases the target is for $<100\text{ms}$ latency, while for some applications it is $<10\text{ms}$ [5, Table 1]. In part, this reflects the fact that low delay is already coming to the fore in network services. For example, Amazon estimates that a 100ms increase in delay reduces its revenue by 1% [6], Google measured a 0.74% drop in web searches when delay was artificially increased by 400ms [7] while Bing saw a 1.2% reduction in per-user revenue when the service delay was increased by 500ms [8]. But the requirement for low latency also reflects the needs of next generation applications such as augmented reality and the tactile internet.

In the present paper we focus on situations where the last hop in Figure 1 is a modern WLAN and is the bot-

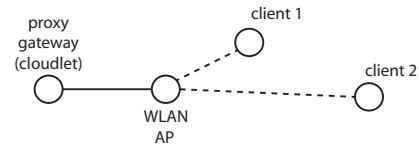


Fig. 1. Schematic of a cloudlet-based edge transport architecture.

tleneck. Key to our work is the ubiquity of aggregation in modern WLANs. Intuitively, the level of aggregation achieved is coupled to queueing. Namely, when only a few packets are queued then there are not enough to allow large aggregated frames to be assembled for transmission. Conversely, when there is a persistent queue backlog then there is a plentiful supply of packets and large frames can be consistently assembled. We show that regulating the send rate to a station so as to maintain an appropriate fixed aggregation level can be used to realise high rate, low delay communication. We then extend consideration to multiple stations. This requires characterising the rate region of WLANs with aggregation, which is highly non-trivial due to the strong coupling between aggregation and queueing. We develop an approximate model, verify its accuracy using experimental measurements and use this to derive a low-delay rate region for WLANs with aggregation. Fortunately, this low delay region is convex and so standard utility-fair optimisation approaches can be used to derive a low delay proportional fair rate allocation. We show how this rate allocation can be implemented at the transport layer on commodity hardware and evaluate performance in an experimental testbed located in a realistic office radio environment.

In summary, our main contributions are as follows: (i) we establish that regulating send rate so as to maintain a target aggregation level can be used to realise high rate, low delay communication over modern WLANs, (ii) we derive a low delay rate region, show that it is convex and derive the low delay proportional fair rate allocation, (iii) we present a prototype transport layer implementation of this low delay rate allocation and evaluate its performance in a realistic

• F. Gringoli is with University of Brescia, Italy.
• D. J. Leith is with Trinity College Dublin, Ireland.

office radio environment.

1.1 Related Work

In recent years there has been an upsurge in interest in userspace transports due to their flexibility and support for innovation combined with ease of rollout. This has been greatly facilitated by the high efficiency possible in userspace with the support of modern kernels. Notable examples of new transports developed in this way include Google QUIC [2], UDT [9] and Coded TCP [3], [10], [11]. ETSI has also recently set up a working group to study next generation protocols for 5G [1]. The use of performance enhancing proxies, including in the context of WLANs, is also not new e.g. RFC3135 [12] provides an entry point into this literature. However, none of these exploit the use of aggregation in WLANs to achieve high rate, low delay communication.

Interest in using aggregation in WLANs pre-dates the development of the 802.11n standard in 2009 but has primarily focused on analysis and design for wireless efficiency, managing loss etc. For a recent survey see for example [13]. The literature on throughput modelling of WLANs is extensive but much of it focuses on so-called saturated operation, where transmitters always have a packet to send, see for example [14] for early work on saturated throughput modelling of 802.11n with aggregation. When stations are not saturated (so-called finite-load operation) then for WLANs which use aggregation (802.11n and later) most studies resort to the use of simulations to evaluate performance due to the complex interaction between arrivals, queueing and aggregation with CSMA/CA service. Notable exceptions include [15], [16] which adopt a bulk service queueing model that assumes a fixed, constant level of aggregation and [17] which extends the finite load approach of [18] for 802.11a/b/g but again assumes a fixed level of aggregation.

Similarly, while utility fair optimisation has previously been considered for WLANs, e.g. [19], [20], [21] this has either ignored aggregation or confined consideration to solutions where only full-sized frames are transmitted (since this maximises throughput when there is freedom to adjust the transmission attempt probability, e.g. see [20] which considers use of TXOP bursting rather than frame aggregation but this just changes the overhead calculations involved).

2 PRELIMINARIES

2.1 Notation

\mathbf{x} denotes a vector and x_i the i 'th element of the vector. Superscript \tilde{x} denotes $\log x$. μ_N denotes the expected value $E[N]$ of random variable N

2.2 Aggregation in 802.11n, 802.11ac etc

A feature shared by all new WLAN standards since around 2009 (when 802.11n was introduced) has been the use of aggregation to amortise PHY and MAC framing overheads across multiple packets. This is essential for achieving high throughputs. Since PHY overheads in particular are largely of fixed duration increasing data rates reduce the time spent to transmit the frame payload but leave the PHY

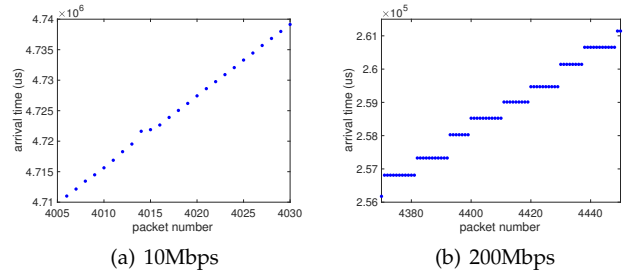


Fig. 2. Illustrating timestamp measurements for UDP packets transmitted via aggregated frames. Two stations, same downlink send rate to both, 802.11ac.

overhead unchanged. Hence, the efficiency, as measured by the ratio of the time spent transmitting user data to the time spent transmitting an 802.11 frame, decreases as data rates increase unless the frame payload is also increased i.e. several user packets are aggregated and transmitted in a single frame.

Since the packets aggregated in a frame share the same destination station (at least in current 802.11 standards), aggregation effectively requires that per station queueing be used at the WLAN access point. When few packets are queued then there are insufficient packets available to allow large aggregated frames to be assembled for transmission. While the scheduler might delay transmission in anticipation of more packets arriving it is known that this is generally not advantageous, e.g. see [14], and we see no evidence of this in our experimental measurements. When the network is lightly loaded then such delay merely increases latency, while as the network load increases queue backlogs start to develop and the level of aggregation naturally increases [14].

2.3 Measuring Aggregation

The level of aggregation can be readily measured at a receiver using packet timestamps. Namely, a timestamp is typically added by the NIC to each packet recording the time when it is received. When a frame carrying multiple packets is received then those packets have the same timestamp and so this can be used to infer which packets were sent in the same frame. For example, Figure 2 shows measured packet timestamps for two different send rates. The setup consists of Linux server (running Debian Jessie) sending UDP packets using iperf 2.0.5 to two Linux clients (running Debian Stretch and with Broadcom BCM4360 802.11ac NICs) via an Asus RT-AC86U Access Point (which uses a Broadcom 4366E chipset). Note that unless otherwise stated we also use this same setup when presenting experimental measurements in the rest of this paper. It can be seen from Figure 2(a) that when the UDP arrival rate at the AP is relatively low each received packet has a distinct timestamp whereas at higher arrival rates, see Figure 2(b), packets start to be received in bursts having the same timestamp. This behaviour reflects the use by the AP of aggregation at higher arrival rates, as confirmed by inspection of the radio headers in the corresponding tcpdump data.

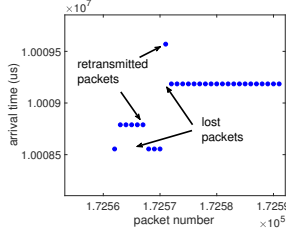


Fig. 3. Illustrating impact of packet loss on timestamp measurements for UDP packets transmitted via aggregated frames. Two stations, 200Mbps downlink send rate to both, 802.11ac.

2.4 Measuring Link Layer Loss/Retransmission

We note that aggregation, when combined with indexing of the packets e.g. by inserting a unique sequence number into the payload of each packet, also allows inference of link layer losses and retransmission since retransmissions result in out of order delivery. This is illustrated by the measurements in Figure 3, which plot receiver timestamp vs packet sequence number. Packets transmitted in the same frame have the same timestamp, so this figure shows the packets from four frames. In the first frame a burst of five packets are not received and are retransmitted in the second frame. In the third frame the first packet is lost and retransmitted by itself in the fourth frame. Note that even without the use of timestamps the reordering of the packets by itself can be used to infer loss and retransmission.

3 LOW DELAY OPERATION

To provide high rate, low latency communication for next generation 5G services we would like to select a downlink send rate which is as high as possible yet ensures that a persistent queue backlog does not develop at the AP. While measurements of round-trip time might be used to estimate the onset of queueing and adjust the send rate, it is known that this can be inaccurate when there is queueing in the reverse path. Accurately measuring one-way delay is also known in general to be challenging¹. In contrast, the number of packets aggregated in a frame is relatively easy to measure accurately and reliably at the receiver, as already noted.

3.1 Inferring Queueing From Level of Aggregation

Intuitively, the level of aggregation used in downlink transmissions to a station is coupled to the queue backlog at the AP of packets destined to the station. When few packets are queued then there are insufficient packets available to allow large aggregated frames to be assembled for transmission. Conversely, when the queue is persistently large then packets are available to be aggregated into large frames. This behaviour can, for example, be seen in the experimental measurements shown in Figure 4. Figure 4(a) shows a time history of number of packets aggregated in each frame and

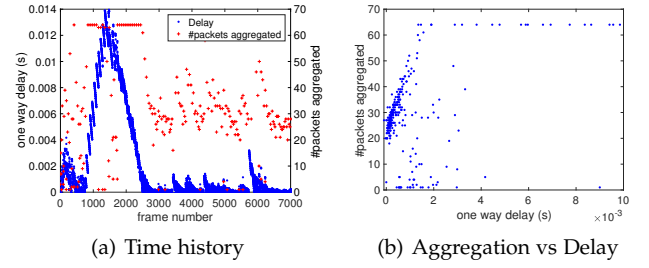


Fig. 4. Measured queueing delay and frame aggregation. Single downlink flow 400Mbps, 802.11ac

the mean one-way delay² experienced by packets sharing the same frame. It can be seen that the delay rises for frames 1000-2500 and that there is a corresponding increase in the number of packets aggregated in these frames to the maximum permitted value of $N_{max} = 64$. Figure 4(b) shows the same data, replotted as aggregation level vs delay. Although the relationship is a noisy one, it can be seen that the aggregation level indeed tends to rise with the delay until it hits the maximum allowed value.

3.2 Controlling Delay

The above observation motivates us to explore whether queueing delay at the AP can be controlled by regulating the packet arrival rate into the AP so as to maintain a specified level of aggregation.

We proceed by introducing a simple feedback loop to adjust the sender transmit rate (corresponding to the AP arrival rate, assuming no losses between sender and AP). Namely, time is partitioned into slots of duration Δ seconds and we let $\mathcal{T}_{i,k}$ denote the set of frames transmitted to station i in slot k . Station i measures the number of packets $N_{i,f}$ aggregated in frame f and reports the average $\hat{\mu}_{N_i}(k) := \frac{1}{|\mathcal{T}_{i,k}|} \sum_{f \in \mathcal{T}_{i,k}} N_{i,f}$ back to the sender. The sender then uses proportional feedback to increase its transmit rate x_i if the observed aggregation level $\hat{\mu}_{N_i}(k)$ is less than the target value N_ϵ and decrease it if $\hat{\mu}_{N_i}(k) > N_\epsilon$. This can be implemented using the pseudo-code shown in Algorithm 1. The stability of this feedback loop is analysed in Section 6.1.1.

Algorithm 1 Feedback loop adjusting transmit rate to regulate aggregation level.

```

 $k = 1$ 
while 1 do
   $\hat{\mu}_{N_i} \leftarrow \frac{1}{|\mathcal{T}_{i,k}|} \sum_{f \in \mathcal{T}_{i,k}} N_{i,f}$ 
   $x_i \leftarrow x_i - K(\hat{\mu}_{N_i} - N_\epsilon)$ 
   $k \leftarrow k + 1$ 
end while

```

We implemented this feedback loop in the testbed setup described in Section 2 and Figure 5 shows experimental

1. The impact of clock offset and skew between sender and receiver applies to all network paths. In addition, when a wireless hop is the bottleneck then the transmission delay can also change significantly over time depending on the number of active stations e.g. if a single station is active and then a second station starts transmitting the time between transmission opportunities for the original station may double.

2. Sender and receiver clocks are synchronised using NTP and we confirmed that clock skew between devices is minor over the duration of the experiment. One way delay is measured by sender inserting the current time into the packet payload immediately before making a socket call to transmit the packet, the receiver then compares this time with the time when the packet is received by the kernel.

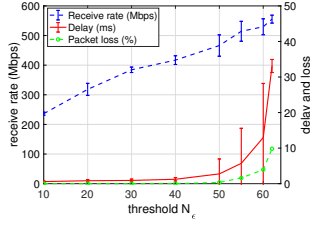


Fig. 5. Measured rate, delay and loss vs target aggregation level N_ϵ . $K = 1$, $\Delta = 1000ms$, 802.11ac with $N_{max} = 64$. Each data point summarises 250s of measurements.

measurements of the client station receive rate (i.e. after any packet loss), one-way delay and packet loss (measured at the transport layer, so after any link layer retransmissions) as the target aggregation level N_ϵ is varied. Also shown are error bars indicating one standard deviation. Note that losses due to decoding errors were always recovered by retransmissions at the link-layer, thus packet loss is associated only with queue overflow within the AP. It can be seen that, as expected, for aggregation levels close to the upper limit $N_{max} = 64$ the delay and loss rise rapidly with N_ϵ . However, when the aggregation is regulated to a lower level, less than about 40 packets, the delay is consistently low and there are no queue overflow losses.

Observe also in Figure 5 that the receive rate increases roughly linearly with N_ϵ . Recall that the rate is regulated to maintain the target aggregation level N_ϵ . Recall that service of the AP queue is stochastic in nature due to the random nature of the contention process used in 802.11 and we can expect this to induce a fluctuating queue backlog and so influence the aggregation level. Further, while iperf 2.0.5 uses packet pacing, this is only approximate and the packet transmissions are still somewhat bursty. Hence, it is perhaps unsurprising that a lower rate is required in order to maintain a lower aggregation level. For N_ϵ around 30 or 40, which as already noted ensures low delay, the rate is around 80% of the maximum.

4 WLAN CAPACITY WITH AGGREGATION

The results in Section 3 indicate that it is indeed possible to ensure high-rate, low delay operation. However, when transmitting to multiple stations then we have to jointly select the transmit rates to all of the stations since wireless is a shared medium. Further, many combinations of transmit rates can all yield low delay. Hence, to proceed we need to characterise the downlink rate region.

4.1 Modelling Aggregation

Consider downlink transmissions in a WLAN (so no collisions) with n client stations indexed by $i = 1, 2, \dots, n$. Index the packets sent by station i by $k = 1, 2, \dots$. These packets are transmitted within 802.11 frames. Index these frames by $f = 1, 2, \dots$ and let $\mathcal{F}_{i,f} \subset \{1, 2, \dots\}$ denote the set of packets aggregated within frame f transmitted to station i and $N_{i,f} = |\mathcal{F}_{i,f}|$ the number of packets aggregated. Since a minimum of one packet must be contained within a frame and a maximum of N_{max} (typically 32 or 64) then $1 \leq N_{i,f} \leq N_{max}$. Assume, for simplicity, that all packets

are of length L bits (this can be easily relaxed), let x_i denote the rate in packets/sec at which packets arrive for transmission to station i , $i = 1, \dots, n$ and $\mathbf{x} = (x_1, \dots, x_n)^T$ the vector of arrival rates.

To model the aggregation behaviour we proceed as follows. The airtime used by frame f transmitted to station i is given by

$$T_{air,i,f} := T_{oh} + \frac{L}{R_{i,f}} N_{i,f} \quad (1)$$

where $R_{i,f}$ is the PHY rate used to transmit the payload of frame f to station i and T_{oh} is the combined time used by MAC and PHY framing plus transmission of the ACK by the receiver. Assume $N_{i,f}$ and $R_{i,f}$ are independent and vary in an i.i.d. manner across frames³. Letting $\mu_{N_i}(\mathbf{x}) = E[N_{i,f}|\mathbf{x}]$ denote the average number of packets transmitted per frame (often we will drop the \mathbf{x} to streamline notation) and $\mu_{R_i} := 1/E[\frac{1}{R_{i,f}}]$ (note that in general⁴ $E[\frac{1}{R_{i,f}}] \neq 1/E[R_{i,f}]$) then the average time between the transmissions by a station is

$$\delta = \sum_{j=1}^n T_{acc} + T_{oh} + \frac{L}{\mu_{R_j}} \mu_{N_j} \quad (2)$$

where T_{acc} is mean airtime used per frame for CSMA/CA contention by the AP (recall that there are no collisions since we consider the downlink only) and we assume that the AP uses a scheduler which, on average, transmits to clients in round-robin fashion. We can rewrite δ equivalently in vector form as

$$\delta = c + \mathbf{w}^T \boldsymbol{\mu}_N \quad (3)$$

where $c = n(T_{acc} + T_{oh})$, $\boldsymbol{\mu}_N = (\mu_{N_1}, \dots, \mu_{N_n})^T$, $\mathbf{w} = (\frac{L}{\mu_{R_1}}, \dots, \frac{L}{\mu_{R_n}})^T$.

During this time on average $x_i \delta$ packets arrive at station i and, assuming the queue is not persistently growing, we need

$$\mu_{N_i} = \Pi \circ x_i \delta = \Pi \circ x_i (c + \mathbf{w}^T \boldsymbol{\mu}_N), \quad i = 1, \dots, n \quad (4)$$

where operator $\Pi \circ z := \max\{1, \min\{N_{max}, z\}\}$ projects z onto interval $[1, N_{max}]$. This gives n equations in n unknowns μ_{N_i} , $i = 1, \dots, n$ that we can solve to estimate the μ_{N_i} . For example, when all stations have same MCS rate $\mu_{R_j} = \mu_R$ and arrival rate $x_j = x$, then by symmetry aggregation is the same at all stations $\mu_{N_i} = \mu_N$ and

$$\mu_N = \Pi \circ x(c + n\mathbf{w}) = \Pi \circ \frac{cx}{1 - nxw} \quad (5)$$

where $w := \frac{L\mu_N}{\mu_R}$. Note that $1 - nxw > 0$ is a necessary condition for the queue not to be persistently growing.

Figure 6 illustrates the aggregation behaviour predicted by this model using 802.11ac MAC parameter values similar

3. Variations in $N_{i,f}$ across frames arise due to fluctuations in the time between transmission opportunities as a result of the stochastic nature of the 802.11 MAC (when the time is longer then it is likely that more packets have arrived and $N_{i,f}$ is larger at the next txop, conversely $N_{i,f}$ tends to be smaller when the time is shorter) and also due to bustiness of packet arrivals. Variations in $R_{i,f}$ primarily arise due to channel fluctuations. Hence, assuming independence of $N_{i,f}$ and $R_{i,f}$ seems reasonable and is also consistent with our experimental measurements.

4. Indeed, to first-order $E[\frac{1}{R_{i,f}}] \approx \frac{1}{E[R_{i,f}]} + \frac{\text{Var}(R_{i,f})}{E[R_{i,f}]^3}$

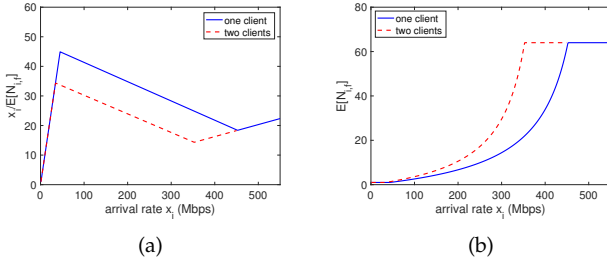


Fig. 6. Mean number $\mu_{N_i} = E[N_{i,f}|\mathbf{x}]$ of packets aggregated in a frame vs arrival rate x_i . At arrival rate X_1 multiple packets start to be aggregated into each frame and at rate X_2 the upper limit N_{max} on the number of packets that can be aggregated in a frame is reached. Theory model, one and two client stations, 802.11ac MAC parameter values.

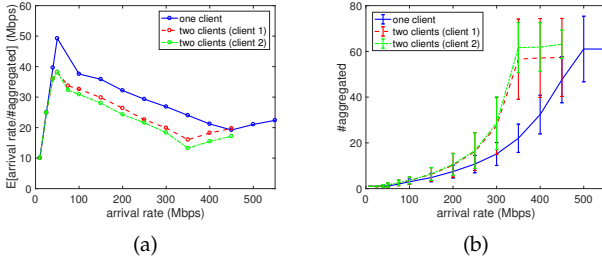


Fig. 7. Number $N_{i,f}$ of packets aggregated in a frame vs arrival rate x_i and number of client stations. Experimental measurements, 802.11ac AP, MAC timestamps.

to those in our experimental measurements below⁵ When the arrival rate is low (below the rate marked X_1 in the figure), then only a single packet is transmitted in each frame, $\mu_{N_i} = 1$ and x_i/μ_{N_i} increases linearly with x_i . Once the arrival rate becomes sufficiently high then multiple packets are aggregated in each frame. The mean per packet overhead is $T_{oh}E[x_i/N_{i,f}|\mathbf{x}] \approx T_{oh}x_i/\mu_{N_i}$, and since x_i/μ_{N_i} decreases as rate x_i increases then the overhead also decreases. Eventually, as the arrival rate increases further still then the maximum aggregation limit N_{max} is reached and $x_i/\mu_{N_i} = x_i/64$ again increases linearly with x_i , albeit at a slower rate.

To help validate this model we collected experimental 802.11ac measurements of aggregation behaviour as the arrival rate and number of client stations is varied, see Figure 7. Comparing with Figure 6 it can be seen that the experimentally measured behaviour is qualitatively the same as the model, although the numerical values match up only approximately. The latter is to be expected since the real measurements include packet loss, a channel which is shared with other networks etc that are neglected by the model. However, qualitative agreement will prove enough for use of the model in our optimisation formulation later since this will make use of measurements to estimate the curve.

⁵ $9\mu s$ slots, $CW_{min} = 15$, $DIFS = 34\mu s$ giving $T_{acc} \approx 106\mu s$; three streams, 80Mhz channel, short GI giving $T_{oh} \approx 108\mu s$ and $\mu_R \approx 513$ Mbps for station 1 and $\mu_R \approx 850$ Mbps for station 2; $L = 1500B$ of which 1470B is useful payload, $N_{max} = 64$.

4.2 Convexity

Ignoring, for the moment, the projection onto interval $[1, N_{max}]$, we can rewrite (4) as

$$\mu_N = (c + w^T \mu_N) \mathbf{x} \quad (6)$$

Lemma 1 (Mean Frame Rate). *Let μ_N be a solution to (6) for arrival rates \mathbf{x} . Then $\frac{x_i}{\mu_{N_i}} = (1 - w^T \mathbf{x})/c$ is a linear function of \mathbf{x} .*

Proof. From (6),

$$\frac{x_i}{\mu_{N_i}} = \frac{1}{c + w^T \mu_N} \quad (7)$$

Also from (6),

$$w^T \mu_N = (c + w^T \mu_N) w^T \mathbf{x} \quad (8)$$

Rearranging (8) yields

$$w^T \mu_N = \frac{cw^T \mathbf{x}}{1 - w^T \mathbf{x}} \quad (9)$$

and substituting this into (7) we have

$$\frac{x_i}{\mu_{N_i}} = \frac{1}{c + \frac{cw^T \mathbf{x}}{1 - w^T \mathbf{x}}} = \frac{1 - w^T \mathbf{x}}{c} \quad (10)$$

The claimed result now follows immediately. \square

Lemma 2 (Mean Aggregation Level). *Let μ_N be a solution to (6) for arrival rates \mathbf{x} . Then $\mu_N = \frac{c\mathbf{x}}{1 - w^T \mathbf{x}}$. Further, μ_{N_i} , $i = 1, \dots, n$ is a convex function of $\tilde{\mathbf{x}} = (\log x_1, \dots, \log x_n)^T$ on the domain $w^T e^{\tilde{\mathbf{x}}} < 1$.*

Proof. By Lemma 1, $\frac{x_i}{\mu_{N_i}} = \frac{1 - w^T \mathbf{x}}{c}$. That is, $\mu_{N_i} = \frac{cx_i}{1 - w^T \mathbf{x}}$, i.e.

$$\mu_N = \frac{c\mathbf{x}}{1 - w^T \mathbf{x}} \quad (11)$$

as claimed. It can be verified by substituting this into (6) that it is indeed a solution.

Turning now to convexity, letting $\tilde{x}_i = \log x_i$ and $\tilde{\mu}_{N_i} = \log \mu_{N_i}$ then it follows from (4) that

$$\tilde{\mu}_{N_i} = \log c + \tilde{x}_i - \log(1 - \sum_{i=1}^n w_i e^{\tilde{x}_i}) \quad (12)$$

It can be verified by inspection of its first and second derivatives that $-\log(1 - z)$ is convex and increasing for $z < 1$ (the first derivative is $1/(1 - z)$ and the second $1/(1 - z)^2$). Since the exponential is convex we have that $\sum_{i=1}^n w_i e^{\tilde{x}_i}$ is a convex function of $\tilde{x}_1, \dots, \tilde{x}_n$. Composing these functions it follows from [22, p84] that $-\log(1 - \sum_{i=1}^n w_i e^{\tilde{x}_i})$ is convex in $\tilde{x}_1, \dots, \tilde{x}_n$ for $w^T e^{\tilde{\mathbf{x}}} = \sum_{i=1}^n w_i e^{\tilde{x}_i} < 1$. The remaining terms in (12) are linear in $\tilde{x}_1, \dots, \tilde{x}_n$ and so convex, hence $\tilde{\mu}_{N_i}$ is a convex function of $\tilde{x}_1, \dots, \tilde{x}_n$. Now $\mu_{N_i} = e^{\tilde{\mu}_{N_i}}$ with e^z convex and increasing in z and $\tilde{\mu}_{N_i}$ is convex in $\tilde{\mathbf{x}}$. Hence, the composition $e^{\tilde{\mu}_{N_i}}$ of e^z with $\tilde{\mu}_{N_i}$ is also convex in $\tilde{\mathbf{x}}$ [22, p84]. That is, μ_{N_i} is convex in $\tilde{\mathbf{x}}$ as stated. \square

Now reinstating the constraint that μ_{N_i} must lie in the interval $[1, N_{max}]$, by Lemma 2 this can be enforced by projecting $\frac{cx_i}{1 - w^T \mathbf{x}}$ onto this interval for each $i = 1, \dots, n$. Similarly, to constrain $\frac{x_i}{\mu_{N_i}}$ by Lemma 1 this can be enforced by projecting $(1 - w^T \mathbf{x})/c$ onto interval $[x_i, \frac{x_i}{N_{max}}]$.

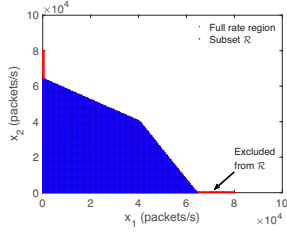


Fig. 8. Illustrating rate region and subset \mathcal{R} (for typical 802.11ac parameter values).

4.3 WLAN Downlink Capacity

The airtime used by a packet $k \in \mathcal{F}_{i,f}$ transmitted to station i within frame f is given by

$$T_{air,i,k} := \frac{T_{oh}}{N_{i,f}} + \frac{L}{R_{i,f}} \quad (13)$$

As already noted, the number $N_{i,f}$ of packets aggregated in the frame and the MCS rate $R_{i,f}$ used are random variables. The expected airtime per second used by transmissions at rate x_i packets per second is therefore given by

$$E[T_{air,i,f} | \mathbf{x}] x_i = T_{oh} E\left[\frac{x_i}{N_{i,f}} | \mathbf{x}\right] + E\left[\frac{L}{R_{i,f}} x_i\right] \quad (14)$$

where the expectation is taken with respect to the variations in $N_{i,f}$ and $R_{i,f}$ across frames, which as already noted we assume are i.i.d. We know from the analysis in earlier sections that the aggregation level $N_{i,f}$ depends on the send rate, hence the use of the conditional expectation. The overall network airtime usage therefore must satisfy

$$\sum_{i=1}^n (T_{acc} + T_{oh}) \frac{x_i}{\mu_{N_i}} + \frac{L}{\mu_{R_i}} x_i \leq 1 \quad (15)$$

where T_{acc} is the time per frame consumed for contention and DIFS. By Lemmas 1 and 2 and the constraint that $1 \leq \mu_{N_i} \leq N_{max}$ it follows that

$$\frac{x_i}{\mu_{N_i}} = \begin{cases} x_i & \mu_{N_i} = \frac{cx_i}{1-\mathbf{w}^T \mathbf{x}} \leq 1 \\ \max\left\{\frac{(1-\mathbf{w}^T \mathbf{x})}{c}, \frac{x_i}{N_{max}}\right\} & \text{otherwise} \end{cases} \quad (16)$$

and so we have the upper bound

$$\frac{x_i}{\mu_{N_i}} \leq \max\left\{\frac{(1-\mathbf{w}^T \mathbf{x})}{c}, \frac{x_i}{N_{max}}\right\} \quad (17)$$

Hence, since $c = n(T_{acc} + T_{oh})$ and $w_i = \frac{L}{\mu_{R_i}}$, the set of rates

$$\mathcal{R} = \{\mathbf{x} : \sum_{i=1}^n \frac{c}{n} \max\left\{\frac{1-\mathbf{w}^T \mathbf{x}}{c}, \frac{x_i}{N_{max}}\right\} + w_i x_i \leq 1\} \quad (18)$$

is admissible, a subset of the full rate region. The full rate region and subset \mathcal{R} are illustrated in Figure 8. It can be seen that \mathcal{R} includes almost all of the rate region apart from the small areas along the two axes corresponding to very low rates for one station. Importantly, unlike the full rate region subset \mathcal{R} is convex since the terms inside the max are both linear in \mathbf{x} , so convex, and composition with the max retains convexity [22, p73], and the term $w_i x_i$ is linear and so convex.

5 LOW DELAY FAIR RATE ALLOCATION

We now embed the foregoing rate and delay constraints within a utility optimisation with the aim of deriving a low-delay rate allocation algorithm suited to use by next generation edge transport protocols. We obtain the following optimisation P ,

$$\max_{\tilde{\mathbf{x}}} \sum_{i=1}^n U(e^{\tilde{x}_i})$$

$$s.t. \sum_{i=1}^n \frac{c}{n} \max\left\{\frac{1-\mathbf{w}^T \mathbf{x}}{c}, \frac{x_i}{N_{max}}\right\} + w_i x_i \leq 1 \quad (19)$$

$$\mu_{N_i}(\tilde{\mathbf{x}}) \leq N_\epsilon, \quad i = 1, \dots, n \quad (20)$$

where $\tilde{x}_i = \log x_i$, $\mu_{N_i}(\tilde{\mathbf{x}}) = \frac{ce^{\tilde{x}_i}}{1-\sum_{j=1}^n w_j e^{\tilde{x}_j}}$ and utility function $U(\cdot)$ is such that $U(e^z)$ is concave in z . Constraint (19) enforces the requirement that the aggregate airtime per second used by transmissions cannot exceed unity. Constraints (20) ensure low delay. The constraints are all convex and the utility is concave, hence optimisation P is convex.

Lemma 3 (Interior of Rate Region). *Suppose $\mu_{N_i}(\tilde{\mathbf{x}}) \leq N_\epsilon \leq N_{max}$. Then $\max\left\{\frac{1-\mathbf{w}^T \mathbf{x}}{c}, \frac{x_i}{N_{max}}\right\} = \frac{1-\mathbf{w}^T \mathbf{x}}{c}$ and constraint (19) is satisfied.*

Proof. Suppose $\mu_{N_i}(\tilde{\mathbf{x}}) \leq N_\epsilon \leq N_{max}$. Then by Lemma 1, $\frac{x_i}{\mu_{N_i}(\tilde{\mathbf{x}})} = \frac{1-\mathbf{w}^T \mathbf{x}}{c} \geq \frac{x_i}{N_{max}}$ and so

$$\max\left\{\frac{1-\mathbf{w}^T \mathbf{x}}{c}, \frac{x_i}{N_{max}}\right\} = \frac{1-\mathbf{w}^T \mathbf{x}}{c} \quad (21)$$

Hence, constraint (19) becomes

$$\sum_{i=1}^n \frac{c}{n} \frac{1-\mathbf{w}^T \mathbf{x}}{c} + w_i x_i \leq 1 \quad (22)$$

But $\sum_{i=1}^n \frac{c}{n} \frac{1-\mathbf{w}^T \mathbf{x}}{c} + w_i x_i = 1 - \mathbf{w}^T \mathbf{x} + \sum_{i=1}^n w_i x_i = 1 - \mathbf{w}^T \mathbf{x} + \mathbf{w}^T \mathbf{x} = 1$. Therefore constraint (19) is always satisfied. \square

Lemma 3 is intuitive. Namely, by not aggregating at the maximum level we do not build up any standing queues at the transmitter and so cannot exceed the network capacity. This also implies that low delay operation comes at the cost of reduced network throughput, as already noted. It follows that selecting $N_\epsilon \leq N_{max}$ then can simplify optimisation P to

$$\max_{\tilde{\mathbf{x}}} \sum_{i=1}^n U(e^{\tilde{x}_i}) \quad s.t. \quad \mu_{N_i}(\tilde{\mathbf{x}}) \leq N_\epsilon \quad (23)$$

for which the Lagrangian is

$$L(\tilde{\mathbf{x}}, \lambda, \mu) = - \sum_{i=1}^n U(e^{\tilde{x}_i}) + \sum_{i=1}^n \lambda_i (\mu_{N_i}(\tilde{\mathbf{x}}) - N_\epsilon) \quad (24)$$

where $\lambda_i, i = 1, \dots, n$ are the multipliers.

5.1 Low Delay Proportional Fair Rate Allocation

In the important case where the utility function $U(\cdot)$ is the log, for which the solution of optimisation P correspond to the proportional fair rate allocation, then it turns out that we can explicitly characterise the solution.

Theorem 1 (Proportional Fair Rate Allocation). *Suppose $N_\epsilon \leq N_{max}$. The the solution to optimisation P is $x_j = \alpha/w_j$ where scaling factor $\alpha = \frac{N_\epsilon w_{max}}{(c+N_\epsilon w_{max}n)} > 0$ with $w_{max} = \max_{i \in \{1, \dots, n\}} w_i$.*

Proof. Since the optimisation is convex (by Lemmas 1 and 2) the KKT conditions are necessary and sufficient for optimality. Namely, an optimum satisfies

$$\sum_{j=1}^n \lambda_j \frac{\partial \mu_{N_j}}{\partial \tilde{x}_i} = 1, \quad i = 1, \dots, n \quad (25)$$

$$\lambda_i(\mu_{N_i}(\tilde{\mathbf{x}}) - N_\epsilon) = 0, \quad i = 1, \dots, n \quad (26)$$

where $\mu_{N_i} = \frac{cx_i}{1-\mathbf{w}^T \mathbf{x}}$ and $\frac{\partial \mu_{N_i}}{\partial \tilde{x}_i} = \frac{cx_i}{1-\mathbf{w}^T \mathbf{x}} \left(1 + \frac{w_i x_i}{(1-\mathbf{w}^T \mathbf{x})}\right)$, $\frac{\partial \mu_{N_j}}{\partial \tilde{x}_i} = \frac{cx_j w_i x_i}{(1-\mathbf{w}^T \mathbf{x})^2}$. When $x_j = \alpha/w_j$ then

$$\sum_{j=1}^n \lambda_j \frac{\partial \mu_{N_j}}{\partial \tilde{x}_i} = \frac{c\alpha}{1-n\alpha} \left(\frac{\lambda_i}{w_i} + \sum_{j=1}^n \lambda_j \frac{\alpha}{w_j (1-n\alpha)} \right) \quad (27)$$

and

$$\lambda_i(\mu_{N_i}(\tilde{\mathbf{x}}) - N_\epsilon) = \lambda_i \left(\frac{c\alpha/w_i}{1-n\alpha} - N_\epsilon \right) \quad (28)$$

Selecting

$$\lambda_i/w_i = \begin{cases} \gamma := \frac{1}{c} \frac{(1-n\alpha)^2}{1-(n-n_{max})\alpha^2} & w_i = w_{max} \\ 0 & w_i < w_{max} \end{cases} \quad (29)$$

where $n_{max} = |\{i \in \{1, \dots, n\} : w_i = w_{max}\}| \geq 1$ is the number of stations with maximal w_i , then

$$\sum_{j=1}^n \lambda_j \frac{\partial \mu_{N_j}}{\partial \tilde{x}_i} = \gamma c \frac{1 - (n - n_{max})\alpha^2}{(1 - n\alpha)^2} = 1 \quad (30)$$

and so condition (25) is satisfied. Further, for the stated choice of α we have that $\frac{c\alpha/w_{max}}{1-n\alpha} = N_\epsilon$. Hence $\lambda_i(\mu_{N_i}(\tilde{\mathbf{x}}) - N_\epsilon) = 0$ for all $i = 1, \dots, n$ and so by (28) complementary slackness condition (26) is also satisfied. The stated conclusion now follows. \square

Observe that the proportional fair rate allocation assigns a rate to station i that is proportional to its mean MCS/PHY rate μ_{R_i} since $1/w_i = \mu_{R_i}/L$. That is, stations with a better channel are allowed to send at a higher rate. Proportional fair rate allocations are not always equal airtime allocations, for example this is not the case in WLANs with MU-MIMO [21]. However, in the the present case this does indeed hold:

Corollary 1 (Equal Airtime). *The proportional fair rate allocation assigns equal mean airtime to every client station.*

Proof. The mean air time used by station i is given by $T_i = \frac{c}{n} \frac{x_i}{\mu_{N_j}} + w_i x_i$, see (15). Substituting the proportional fair solution from Theorem 1, $T_i = \frac{c}{n} \frac{\alpha}{w_i \mu_{N_j}} + \alpha$. By Lemma 2, $\mu_{N_i} = \frac{cx_i}{1-\mathbf{w}^T \mathbf{x}}$ and using this in the expression for T_i and rearranging yields $T_i = 1/n$. This holds for all $i \in \{1, \dots, n\}$. \square

While the airtime used by each station is equal, stations with different channels operate with different aggregation levels, with transmissions on channels with a higher mean MCS/PHY rate having a higher aggregation level than transmissions on channels with a low MCS/PHY rate:

Corollary 2 (Different Aggregation Levels). *With a proportional fair rate allocation the mean aggregation level μ_{N_i} of transmissions to station i is proportional to the mean MCS/PHY rate μ_{R_i} , namely $\mu_{N_i} = \frac{c\alpha}{1-n\alpha} \frac{\mu_{R_i}}{L}$.*

Proof. By Lemma 2, $\mu_{N_i} = \frac{cx_i}{1-\mathbf{w}^T \mathbf{x}}$. Substituting the proportional fair solution from Theorem 1 it follows that $\mu_{N_i} = \frac{1}{w_i} \frac{c\alpha}{1-n\alpha}$. Now recall that $1/w_i = \mu_{R_i}/L$. \square

As discussed in more detail in Section 6, the proportional lends itself to implementation using easily measured quantities.

5.2 Other Utility Functions

When the Slater condition is satisfied then strong duality holds and we can find an optimum by dual ascent,

$$\tilde{\mathbf{x}}(k+1) \in \arg \min_{\tilde{\mathbf{x}}} L(\tilde{\mathbf{x}}, \boldsymbol{\lambda}(k)) \quad (31)$$

$$\lambda_i(k+1) = [\lambda_i(k) + \alpha(\mu_{N_i}(\tilde{\mathbf{x}}(k)) - N_\epsilon)]^+ \quad (32)$$

where $\alpha > 0$ is the step size. The Lagrangian is not separable since the expression for μ_{N_i} is coupled to all of the arrival rates \tilde{x}_j , $j = 1, \dots, n$.

Let $\hat{\mu}_{N_i}(k)$ be the empirical average of the number of packets aggregated in the frames sent between dual updates k and $k+1$. Replace μ_{N_i} with $\hat{\mu}_{N_i}(k)$ in the update and note that $E[\hat{\mu}_{N_i}(k)|\tilde{\mathbf{x}}(k)] = \mu_{N_i}(\tilde{\mathbf{x}}(k))$ since the $N_{i,f}$ are assumed i.i.d given fixed arrival rate $\mathbf{x}(k)$. This yields the following approximate update,

$$\tilde{\mathbf{x}}(k+1) \in \arg \min_{\tilde{\mathbf{x}}} L(\tilde{\mathbf{x}}, \boldsymbol{\lambda}(k)) \quad (33)$$

$$= \arg \min_{\tilde{\mathbf{x}}} - \sum_{i=1}^n U(e^{\tilde{x}_i}) + \sum_{i=1}^n \lambda_i \hat{\mu}_{N_i}(\tilde{\mathbf{x}}) \quad (34)$$

$$\lambda_i(k+1) = [\lambda_i(k) + \alpha(\hat{\mu}_{N_i}(k) - N_\epsilon)]^+ \quad (35)$$

Observe that by replacing $\mu_{N_i}(\tilde{\mathbf{x}}(k))$ by the observations $\hat{\mu}_{N_i}(k)$ we implicitly evaluate $\mu_{N_i}(\tilde{\mathbf{x}}(k)) = \frac{ce^{\tilde{x}_i}}{1 - \sum_{j=1}^n w_j e^{\tilde{x}_j}}$. By avoiding explicit evaluation we do not need to know the w_j parameter values, to guarantee convergence its enough that we know the relationship is convex. By construction we have $E[\hat{\mu}_{N_i}(k)|\tilde{\mathbf{x}}(k)] = \mu_{N_i}(\tilde{\mathbf{x}}(k))$. Applying Theorem 1 of [23], then this update will converge in expectation to a solution of the original problem..

6 PERFORMANCE EVALUATION

To evaluate performance under realistic network conditions (our testbed is located in an office environment in the University of Brescia where the unlicensed channels are shared by many networks and heavily used), we implemented the low delay proportional fair rate allocation in Theorem 1 in our 802.11ac experimental testbed.

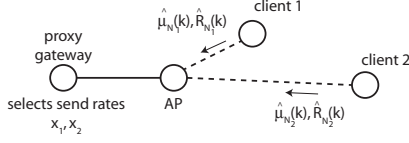


Fig. 9. Schematic of scheduler architecture. Clients send reports of observed aggregation level and MCS rate to proxy which then uses this information to adjust the downlink send rate to each station.

6.1 Prototype Implementation

We build on the simple feedback loop in Algorithm 1. Time is partitioned into slots of duration Δ seconds and $\mathcal{T}_{i,k}$ denotes the set of frames transmitted to station i in slot k . Client stations measure⁶ $N_{i,f}$ and $R_{i,f}$ and report the averages $\hat{\mu}_{N_i}(k) := \frac{1}{|\mathcal{T}_{i,k}|} \sum_{f \in \mathcal{T}_{i,k}} N_{i,f}$ and $\hat{\mu}_{R_i}(k) := \frac{1}{|\mathcal{T}_{i,k}|} \sum_{f \in \mathcal{T}_{i,k}} R_{i,f}$ back to a server which then uses this information to select the downlink send rates \mathbf{x} to the clients. Recall that we are considering next generation edge transports and so this server would typically be located in the cloud close to the network edge. While it may be located on the wireless access point this is not essential, and indeed we demonstrate this feature in all of our experiments by making use of a proprietary closed access point. This software architecture is illustrated in Figure 9.

The server uses a proportional feedback loop to adjust the vector of downlink send rates \mathbf{x} . Namely, it increases the rate x_{i^*} of the station i^* with highest MCS rate $\hat{\mu}_{R_i}(k)$ when its observed aggregation level $\hat{\mu}_{N_i}(k)$ is less than the target value N_ϵ and decreases x_{i^*} when $\hat{\mu}_{N_i}(k) > N_\epsilon$, i.e. at slot k

$$x_{i^*}(k+1) = x_{i^*}(k) - K(\hat{\mu}_{N_i}(k) - N_\epsilon) \quad (36)$$

where feedback gain K is a design parameter. The rates of the other stations are then assigned proportionally,

$$x_i(k+1) = x_{i^*}(k+1) \frac{\hat{\mu}_{R_j}}{\hat{\mu}_{R_{i^*}}}, \quad i = 1, \dots, n \quad (37)$$

Pseudo code for this update is shown in Algorithm 2.

Algorithm 2 Pseudo code for proportional fair rate controller

```

 $k = 1$ 
while 1 do
   $\hat{\mu}_{N_i} \leftarrow \frac{1}{|\mathcal{T}_{i,k}|} \sum_{f \in \mathcal{T}_{i,k}} N_{i,f}, \hat{\mu}_{R_i} \leftarrow \frac{1}{|\mathcal{T}_{i,k}|} \sum_{f \in \mathcal{T}_{i,k}} R_{i,f}$ 
   $i^* \in \arg \max_{i \in \{1, \dots, n\}} w_i$ 
   $x_{i^*} \leftarrow x_{i^*} - K(\hat{\mu}_{N_{i^*}} - N_\epsilon)$ 
   $x_j \leftarrow x_{i^*} \frac{\hat{\mu}_{R_j}}{\hat{\mu}_{R_{i^*}}}, j = 1, \dots, n$ 
   $k \leftarrow k + 1$ 
end while

```

Note that this update only use readily available observations. Namely, the frame aggregation level $N_{i,f}$ and the MCS rate $R_{i,f}$, both of which can be observed in userspace by packet sniffing on client i . While we relied on a model to

6. Note that the proportional fair rate allocation ensures that the send rate to every station is non-zero i.e. no station is starved, see Theorem 1. Hence each station always receives packets and is able to estimate $\hat{\mu}_{N_i}(k)$ and $\hat{\mu}_{R_i}(k)$.

establish convexity and the form of the low delay proportional fair rate allocation, no model parameters are needed in order to actually implement Algorithm 2 (apart from the number of stations n that the server allocates rates to, which is known trivially). Design parameters N_ϵ , gain K and update interval Δ do need to be selected. Selection of target aggregation level N_ϵ has already been discussed in detail, with a typical value being $N_\epsilon = 32$, which leaves the feedback gain K and update interval Δ . We investigate these further below but typical values are $K = 1$ and $\Delta = 1000ms$.

6.1.1 Stability Analysis

Before proceeding we briefly comment on the stability of the nonlinear feedback loop :

$$x_i(k+1) = x_i(k) - K(\mu_{N_i}(k) - N_\epsilon) \quad (38)$$

where $\mu_{N_i}(k) = \Pi \circ (\frac{cx_i(k)}{1-w_ix_i(k)})$ by Lemma 2. Note that the actual feedback loop (36) in Algorithms 1 and 2 uses $\hat{\mu}_{N_i}(k)$ rather than $\mu_{N_i}(k)$, which introduces zero mean noise but should not affect stability. Letting x^* denote the rate at which $\mu_{N_i}(k) = N_\epsilon \in (1, N_{max})$ then

$$\left. \frac{d\mu_{N_{x_i}}(k)}{dx_i(k)} \right|_{x_i(k)=x^*} = \frac{c}{(1-w_ix^*)^2} \quad (39)$$

and linearising the dynamics (38) about this point yields,

$$\delta x_i(k+1) \approx (1 - K \frac{c}{(1-w_ix^*)^2}) \delta x_i(k) \quad (40)$$

where $\delta x_i(k) = x_i(k) - x^*$. For stability we require $0 < K \frac{c}{(1-w_ix^*)^2} < 2$ [24], that is,

$$0 < K < 2 \frac{(1-w_ix^*)^2}{c} \quad (41)$$

Recall $w_ix^* = L/\mu_{R_i}x^*$ is the airtime used by the payload of frames sent to station i and $cx^*/N_\epsilon = (T_{acc} + T_{oh})x^*/N_\epsilon$ is the airtime used by the PHY and MAC overheads. We must have $w_ix^* + cx^*/N_\epsilon < 1$ and so $1 - w_ix^* > cx^*/N_\epsilon$ i.e. $2 \frac{(1-w_ix^*)^2}{c} > 2c(x^*/N_\epsilon)^2$. Typical values are $c > 200us$, $N_\epsilon = 32$ and $x^* > 8000$ packets/sec (corresponding to 100Mbps with 1500B packets) giving $K < 12.5$ for stability. Note that this only ensures local stability. While a necessary condition for global stability it is not sufficient and further analysis of the nonlinear dynamics is needed to confirm conditions on K to ensure global stability.

6.2 Experimental Measurements

6.2.1 Tracking Changing Channel Conditions

We begin by presenting measurements in Figure 10 which demonstrate the ability of the feedback loop in Algorithm 2 to adjust the rate allocation to reflect changing channel conditions so as to maintain both low delay and fairness. These measurements are taken during the day in an office environment where the unlicensed channels are shared by many networks and groups of people move about, creating a complex changing radio 5GHz environment (by taking additional measurements at night we confirmed that the channel is indeed stable when these factors are removed).

Station 1 is closer to the AP and so generally has a higher MCS rate than station 2. It can be seen from Figure 10(a)

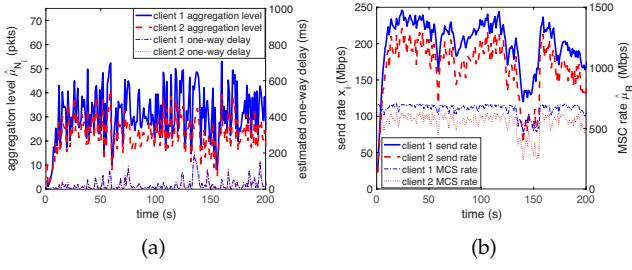


Fig. 10. Experimental measurements illustrating proportional fair rate allocation and adaptation to changing channel conditions to maintain roughly constant aggregation level and so low delay. Two client stations, 802.11ac, $N_e = 32$, $K = 1$, $\Delta = 1000ms$.

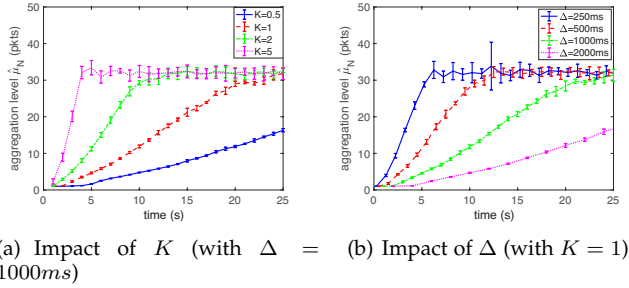


Fig. 11. Convergence rate vs feedback gain K and update interval Δ . Mean and standard deviation from 10 runs at each parameter value. One client, 802.11ac, $N_e = 32$.

that the aggregation level of station 1 is regulated at around the target value of $N_e = 32$ packets, although there are fluctuations due to channel variations etc. It can be seen from Figure 10(b) that the send rates of the stations are roughly proportional to their MCS rates, corresponding to the proportional fair allocation. Adaptation of the send rates to changes in channel conditions is also evident, e.g. around time 140s there is a sharp decrease in the MCS rates of both stations. It can be seen from Figure 10(b) that the send rates adapt to this change in channel conditions, and from Figure 10(a) that, apart from a short spike in delay when the channel initially changes, the delay remains regulated at a low value despite the large changes in channel conditions.

6.2.2 Convergence Rate

We expect that the speed at which the aggregation level and send rate converge to their target values when a station first starts transmitting is affected by the choice of feedback gain K and update interval Δ . Figure 11 plots measurements showing the transient following startup of a station vs the choice of K and Δ . The plots show the average and standard deviation from 10 runs for each choice of parameter value.

It can be seen from Figure 11(a) that as gain K is increased (while holding Δ fixed) the time to converge to the target aggregation level $N_e = 32$ decreases. However, as the gain is increased the feedback loop eventually becomes unstable. Indeed, not shown in the plot is the data for $K = 10$ which shows large, sustained oscillations that would obscure the other data on the plot. Similarly, it can be seen from Figure 11(b) that as the update interval Δ is decreased the convergence time decreases.

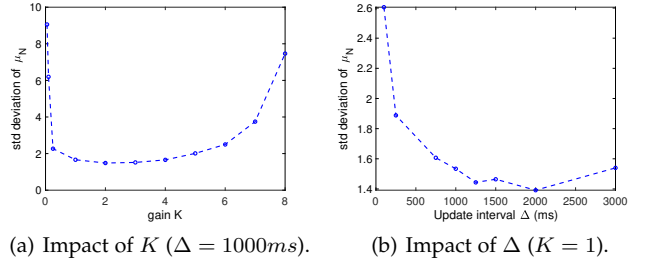


Fig. 12. Noise rejection (as measured by standard deviation of $\hat{\mu}_N$) vs feedback gain K and update interval Δ . One client, 802.11ac.

6.2.3 Disturbance Rejection

Observe in Figure 11 that while the convergence time decreases as K is increased the corresponding error bars indicated on the plots increase. As well as the convergence time we are also interested in how well the controller regulates the aggregation level about the target value N_e . Intuitively, when the gain K is too low then the controller is slow to respond to changes in the channel and the aggregation level will thereby show large fluctuations. The situation when K is increased increased we expect feedback loop is also able to respond more quickly to genuine changes in channel behaviour. However, when the gain is too high it may overreact and so magnify the fluctuations on aggregation level (with instability being an extreme instance of this, see Section 6.1.1). This behaviour can be seen in Figure 12(a) which plots measurements of the standard deviation of the aggregation level $\hat{\mu}_N$ (where the empirical mean is calculated over the update interval Δ of the feedback loop) as the control gain K is varied.

When the the update interval Δ is made smaller we expect that the observations $\hat{\mu}_{N_i}(k)$ and $\hat{\mu}_{R_i}(k)$ will tend to become more noisy (since they are based on fewer frames) which may also tend to cause the aggregation level to fluctuate more. However, the feedback loop is also able to respond more quickly to genuine changes in channel behaviour. Conversely, as Δ increases the estimation noise falls but the feedback loop becomes more sluggish. Figure 12(b) plots measurements of the standard deviation of the aggregation level $\hat{\mu}_N$ as Δ is varied. It can be seen that due to the interplay between these two effects that the standard deviation of $\hat{\mu}_N$ increases when Δ selected too small or too large, with a sweet spot for Δ around 1250-2000ms.

7 ASSUMPTIONS

In this section we review the assumptions used in our analysis, and in particular try to identify those assumptions that can be readily relaxed and those that cannot.

1) *Downlink Only.* We focus on the downlink, as is common in the wireless literature since it typically carries the bulk of traffic. Achieving low delay on the downlink is also the more challenging task for an edge transport since the queue at the AP cannot be directly observed. In contrast, on the uplink traffic shaping can be implemented at the client (e.g. within the app implementing the edge transport layer) thereby making the uplink queue occupancy visible to the transport layer. By communicating this to the proxy it

can then jointly allocate client downlink and uplink rates to ensure low delay and high rate.

2) *Link Layer Losses/Retransmissions Ignored*. The theoretical analysis in Sections 4 and 5 ignores link layer losses and associated retransmissions to streamline the presentation, although of course our experimental measurements include these effects. It is straightforward to extend the analysis to include these by adjusting equation (4) to include retransmissions. The proportional fair solution remains an equal airtime one but the airtime now includes the time consumed by retransmissions.

3) *WLAN is Bottleneck*. We assume that the WLAN is the bottleneck. This is probably reasonable in enterprise edge networks or when the proxy server is co-located with the AP. However, when the proxy is located in the cloud then the bottleneck may well lie in the backhaul path between the AP and the proxy. Our initial measurements (which we plan to report on separately) indicate that observation of the aggregation level can be used to infer the bottleneck location i.e. WLAN or backhaul. This could be then used to restrict application of the approach in the present paper to situations where the WLAN is the bottleneck. That leaves open the question of how to achieve low delay and high rate when the backhaul is the bottleneck, but since this is a major undertaking in its own right we leave this as future work.

4) *Centralised Operation*. Algorithm 2 is centralised in nature, namely clients report measurements to the proxy which then decides on the appropriate downlink send rate for each client. This is a feature of the edge transport architecture considered here, providing the flexibility to create more flexible rate allocation approaches. Standard reformulations, e.g. ADMM or the approach in [23], might be used to solve optimisation P in a distributed fashion at the cost of increased complexity and slower convergence.

8 SUMMARY & CONCLUSIONS

In this paper we establish that regulating send rate so as to maintain a target aggregation level can be used to realise high rate, low delay communication over modern WLANs. Building on this, we derive an approximate throughput model for WLANs with aggregation, use this to determine a convex low delay rate region and so obtain the low delay proportional fair rate allocation. We present a prototype transport layer implementation of this low delay rate allocation and evaluate its performance in a realistic office radio environment.

REFERENCES

- [1] *Next Generation Protocols – Market Drivers and Key Scenarios*. European Telecommunications Standards Institute (ETSI), 2016. [Online]. Available: http://www.etsi.org/images/files/ETSIWhitePapers/etsi_wp17_Next_Generation_Protocols_v01.pdf
- [2] J. Iyengar and I. Swett, “QUIC: A UDP-Based Secure and Reliable Transport for HTTP/2,” *IETF Internet Draft*, 2015. [Online]. Available: <https://tools.ietf.org/html/draft-tsvwg-quic-protocol-00>
- [3] M. Kim, J. Cloud, A. ParandehGheibi, L. Urbina, K. Fouli, D. J. Leith, and M. Medard, “Congestion control for coded transport layers,” in *Proc IEEE International Conference on Communications (ICC)*, 2014, pp. 1228–1234.
- [4] *Open Fast Path*, 2016. [Online]. Available: <http://www.openfastpath.org/>
- [5] *5G White Paper*. Next Generation Mobile Networks (NGMN) Alliance, 2015. [Online]. Available: https://www.ngmn.org/uploads/media/NGMN_5G_White_Paper_V1_0.pdf
- [6] T. Flach, N. Dukkipati, A. Terzis, B. Raghavan, N. Cardwell, Y. Cheng, A. Jain, S. Hao, E. Katz-Bassett, and R. Govindan, “Reducing web latency: the virtue of gentle aggression,” *ACM SIGCOMM Computer Communication Review*, vol. 43, no. 4, pp. 159–170, 2013.
- [7] W. Zhou, Q. Li, M. Caesar, and P. Godfrey, “ASAP: A low-latency transport layer,” in *Proceedings of the Seventh Conference on emerging Networking EXperiments and Technologies*. ACM, 2011, p. 20.
- [8] S. Souders, “Velocity and the bottom line,” in *Velocity (Web Performance and Operations Conference)*, 2009. [Online]. Available: <http://radar.oreilly.com/2009/07/velocity-making-your-site-fast.html>
- [9] Y. Gu and R. L. Grossman, “Udt: Udp-based data transfer for high-speed wide area networks,” *Comput. Netw.*, vol. 51, no. 7, pp. 1777–1799, May 2007. [Online]. Available: <http://dx.doi.org/10.1016/j.comnet.2006.11.009>
- [10] M. Karzand, D. J. Leith, J. Cloud, and M. Medard, “Design of FEC for Low Delay in 5G,” *IEEE Journal Selected Areas in Communications (JSAC)*, vol. 35, no. 8, pp. 1783–1793, 2016.
- [11] A. Garcia-Saavedra, M. Karzand, and D. J. Leith, “Low Delay Random Linear Coding and Scheduling Over Multiple Interfaces,” *IEEE Trans on Mobile Computing*, vol. 16, no. 11, pp. 3100–3114, 2017.
- [12] J. Border, M. Kojo, J. Griner, G. Montenegro, and Z. Shelby, “Performance enhancing proxies intended to mitigate link-related degradations,” Internet Requests for Comments, RFC Editor, RFC 3135, June 2001.
- [13] R. Karmakar, S. Chattopadhyay, and S. Chakraborty, “Impact of IEEE 802.11n/ac phy/mac high throughput enhancements on transport and application protocols: A survey,” *IEEE Communications Surveys Tutorials*, vol. 19, no. 4, pp. 2050–2091, Fourthquarter 2017.
- [14] T. Li, Q. Ni, D. Malone, D. Leith, Y. Xiao, and T. Turletti, “Aggregation with Fragment Retransmission for Very High-Speed WLANs,” *IEEE/ACM Transactions on Networking*, vol. 17, no. 2, pp. 591–604, 2009.
- [15] S. Kuppa and G. Dattatreya, “Modeling and Analysis of Frame Aggregation in Unsaturated WLANs with Finite Buffer Stations,” in *Proc WCNC*, 2006, pp. 967–972.
- [16] B. Bellalta and M. Oliver, “A space-time batch-service queueing model for multi-user mimo communication systems,” in *Proceedings of the 12th ACM International Conference on Modeling, Analysis and Simulation of Wireless and Mobile Systems*, ser. MSWiM ’09. New York, NY, USA: ACM, 2009, pp. 357–364. [Online]. Available: <http://doi.acm.org/10.1145/1641804.1641866>
- [17] B. Kim, H. Hwang, and D. Sung, “Effect of Frame Aggregation on the Throughput Performance of IEEE 802.11n,” in *Proc WCNC*, 2008, pp. 1740–1744.
- [18] D. Malone, K. Duffy, and D. Leith, “Modeling the 802.11 distributed coordination function in nonsaturated heterogeneous conditions,” *IEEE/ACM Trans. Netw.*, vol. 15, no. 1, pp. 159–172, Feb. 2007. [Online]. Available: <http://dx.doi.org/10.1109/TNET.2006.890136>
- [19] A. Checchio and D. J. Leith, “Proportional Fairness in 802.11 Wireless LANs,” *IEEE Communications Letters*, vol. 15, no. 8, pp. 807–809, August 2011.
- [20] —, “Fair Virtualization of 802.11 Networks,” *IEEE/ACM Trans. Netw.*, vol. 23, no. 1, pp. 148–160, Feb. 2015. [Online]. Available: <http://dx.doi.org/10.1109/TNET.2013.2293501>
- [21] V. Valls and D. Leith, “Proportional Fair MU-MIMO in 802.11 WLANs,” *Wireless Communications Letters, IEEE*, vol. 3, no. 2, pp. 221–224, 2014.
- [22] S. Boyd and L. Vandenberghe, *Convex Optimization*. New York, NY, USA: Cambridge University Press, 2004.
- [23] V. Valls and D. J. Leith, “A Convex Optimization Approach to Discrete Optimal Control,” *IEEE Transactions on Automatic Control*, 2018.
- [24] W. J. Rugh, *Linear System Theory*. Pearson, 1995.

PLACE
PHOTO
HERE

Francesco Gringoli received the Laurea degree in telecommunications engineering from the University of Padua, Italy, in 1998 and the Ph.D. degree in information engineering from the University of Brescia, Italy, in 2002. Since 2005, he has been an Assistant Professor of Telecommunications in the Dept. of Information Engineering at the University of Brescia, Italy. He started the OpenFWWF Project in 2009. He is a senior member of the IEEE.

PLACE
PHOTO
HERE

Doug Leith graduated from the University of Glasgow in 1986 and was awarded his PhD, also from the University of Glasgow, in 1989. In 2001, Prof. Leith moved to the National University of Ireland, Maynooth and then in Dec 2014 to Trinity College Dublin to take up the Chair of Computer Systems in the School of Computer Science and Statistics. His current research interests include wireless networks, network congestion control, distributed optimization and data privacy.